

1 **Boosting aerobic microbial protein productivity and quality on brewery**
2 **wastewater: Impact of anaerobic acidification, high-rate process and biomass age**

3

4 Gustavo Papini^a, Maarten Muys^a, Tim Van Winckel^a, Francis A. Meerburg^b, Wannes
5 Van Beeck^a, Pieter Vermeir^c and Siegfried E. Vlaeminck^{a*}

6

7 ^a Research Group of Sustainable Energy, Air and Water Technology, Department of
8 Bioscience Engineering, University of Antwerp, Groenenborgerlaan 171, 2020
9 Antwerpen, Belgium

10 ^b Independent scholar, Dijkstraat 8, 2630 Aartselaar, Belgium

11 ^c Laboratory of Chemical Analysis, Department of Green Chemistry and Technology,
12 Gent University, Valentin Vaerwyckweg 1, 9000 Gent, Belgium

13

14 *Corresponding author e-mail: Siegfried.Vlaeminck@UAntwerpen.be

15

16 Keywords: resource recovery; single-cell protein; fermentation; contact stabilization;
17 aquafeed

18

19 **Abstract**

20 Consortia of aerobic heterotrophic bacteria (AHB) are appealing as sustainable
21 alternative protein ingredient for aquaculture given their high quality, and their
22 production potential on feed-grade industrial wastewater. Today, the impact between
23 pre-treatment, bioprocess choice and key parameter setting on AHB productivity and
24 nutritional properties is unknown. This study investigated for the first time known the
25 effects on AHB microbial protein production from (i) raw vs. anaerobically fermented
26 brewery wastewater, (ii) high-rate activated sludge (HRAS) without vs. with feast-
27 famine conditions, and (iii) three short solids retention times (SRT): 0.25, 0.50 and 1.00
28 d. High biomass (4.4-8.0 g TSS/L/d) and protein productivities (1.9-3.2 g protein/L/d)
29 were obtained while achieving COD removal efficiencies up to 98% at SRT 0.50 d. The
30 AHB essential amino acid (EAA) profiles were above rainbow trout requirements,
31 excluding the S-containing EAA, highlighting the AHB biomass replacement potential
32 for unsustainable fishmeal in salmonid diets.

33 **1. Introduction**

34 The World's population will reach 9.7 billion by 2050 (United Nations, 2019). At the
35 same time, the predicted wealth increase will boost further animal-based protein
36 demand in human diets (Godfray et al., 2010). In this period, fish production is
37 projected to raise 21%, compared to 2018 (FAO, 2020). As virtually all fish stocks are
38 overexploited (Godfray et al., 2010), this demand is expected to be covered by
39 aquaculture (Rana et al., 2009). Nonetheless, aquaculture depends for one third on the
40 limited provision of the increasingly expensive and unsustainable fish meal (FM) (Rana
41 et al., 2009). Thus, alternative protein sources are needed and microbial protein (MP) is
42 considered a promising feed ingredient for aquaculture.

43 MP are microorganisms, such as microalgae, bacteria, yeast or fungi, that have high
44 nutritional quality and can be use as food or feed. They have several environmental
45 benefits compared with traditional protein sources such as: high protein content (up to
46 83%), faster growth, no necessity of arable land, high nutrients assimilation efficiency
47 and virtually nil water usage, as some MP can grow in liquid sidestreams (Verstraete et
48 al., 2016). Most MP applications and developments as feed ingredients are based on
49 dried microbial biomass of non-engineered bacteria, i.e. single-cell protein, which
50 facilitates regulatory and end-user acceptance. Currently, microalgae and methane
51 oxidizing bacteria (MOB) are the main relevant MP being supplied to the feed market
52 (Ritala et al., 2017) but they rely on primary products while MPs production based on
53 secondary resources are still missing. In this context, the most promising microbes are
54 purple non-sulphur bacteria (PNSB), microalgae bacterial floc (MaB) and aerobic
55 heterotrophic bacteria (AHB) (Verstraete et al., 2016). PNSB is a phototrophic
56 anoxygenic microbe that, for wastewater treatment application, grows together with

57 other bacteria reaching growth rates up to 3.7 d^{-1} and yields close to 1 g of chemical
58 oxygen demand (COD) as biomass/g $\text{COD}_{\text{removed}}$ (Alloul et al., 2019). MaB is a
59 synergetic consortia between microalgae (phototrophic) and bacteria (heterotrophic) that
60 have been tested at growth rates below 0.17 d^{-1} (Van Den Hende, 2014). Both MP have
61 similar challenges such as tackling growth restraint due to light scattering and the poor
62 settling properties (Van Den Hende, 2014). AHB are composed of a mixed microbial
63 community that grows easily as flocs (settleable) in the aerobic reactor of the
64 conventional activated sludge (CAS) processes for domestic and industrial wastewater
65 treatment, and can achieve high growth rates and yields, up to 6 d^{-1} and $1 \text{ g COD}_{\text{biomass}}/\text{g}$
66 $\text{COD}_{\text{removed}}$ respectively (Meerburg et al., 2016). Currently, this biomass is considered a
67 waste stream although studies showed positive feeding trial results and that AHB
68 quality is comparable to fish and soybean meal (Vriens et al., 1989). Still, the presence
69 of heavy metals and faecal contamination in some wastewaters raises concerns about its
70 safety. To preserve AHB quality and obtain public acceptability, the use of
71 uncontaminated streams such as wastewater from food and beverage industries is
72 recommended (Verstraete et al., 2016) and the development of a process able to
73 maximize AHB production and quality while treating these streams is required.
74 In order to boost AHB productivities high-rate conventional activated sludge (HiCAS)
75 and the high-rate contact stabilization (HiCS), are more appropriate. Under short SRT
76 ($< 2 \text{ day}$) and high specific loading rate ($> 2 \text{ g COD/g VSS/d}$), they maximize carbon
77 redirection into biomass (Meerburg et al., 2015). The difference between both is that
78 HiCAS only contains one phase, where COD is oxidized under aerobic conditions. In
79 HiCS, a contact phase is included where the incoming substrate meets starved sludge
80 coming from the stabilization step, under absence or low levels of oxygen ($< 0.5 \text{ mg}$

81 O₂/L). After settling, the return sludge is aerated in the stabilizer phase in absence of
82 feed to starve the biomass till returning to the contactor, forming a feast-famine regime
83 (Meerburg et al., 2015). There are several full-scale HiCAS in operation for domestic
84 wastewater treatment (Meerburg et al., 2016), where the biomass is used for energy
85 recovery instead, while HiCS remains a novel approach (Rahman et al., 2019). Here,
86 HiCAS and HiCS were studied as potential AHB production processes.

87 Operational conditions can affect the AHB community composition (Gonzalez-Martinez
88 et al., 2016; Valentín-Vargas et al., 2012), productivity and quality. SRT is one of the
89 main parameters to design AS and shorter SRTs leads to higher observed cell yields
90 (Vriens et al., 1989). Since maximal yield is desired, SRTs below 1 d were chosen to
91 select for fast growing bacteria. Concomitantly, yield, rate of utilization, productivity of
92 MP and microbial community are strongly dependent on the substrate (Fatemeh et al.,
93 2019) which might affect biomass quality. Thus, simpler substrate could favour the
94 growth of specific bacteria and, consequently, impact both productivity and MP quality.

95 There is also a great knowledge gap on understanding the link between process
96 parameters and the composition of the HRAS microbiome. Only two studies using
97 HRAS in sewage treatment provided information about the microbial community
98 (Gonzalez-Martinez et al., 2016; Meerburg et al., 2016). For industrial wastewater
99 treatment and MP production this information is currently inexistent.

100 Hence, this study aims to determine the impact of different substrates, reactor operation
101 and SRTs, to the COD fate in the process, COD removal efficiency, MP productivity,
102 biomass quality, and AHB community composition. Therefore, 12 scenarios were tested
103 using all combinations of substrate (raw and fermented synthetic brewery wastewater),
104 reactor operation (HiCAS and HiCS) and short SRTs (0.25, 0.50 and 1.00 d).

105 **2. Materials and methods**

106 **2.1. Synthetic brewery wastewater**

107 Synthetic raw and fermented wastewater recipes were designed to obtain similar
108 characteristics of the real brewery wastewater before and after fermentation. Synthetic
109 wastewater was used to guarantee reproducibility and prevent the occurrence of
110 confounding factors due to the quality oscillation of the real brewery wastewater.
111 Samples from four Flemish breweries were analysed and data from the literature were
112 gathered in order to define the typical COD speciation, pH and temperature of brewery
113 wastewater, that were then used as target values for the raw synthetic brewery
114 wastewater recipe (Driessen and Vereijken, 2003; Okoli and Okonkwo, 2016). Easily
115 biodegradable organic components such as sugars, soluble starch, volatile fatty acids
116 (VFA), and ethanol are typically present in brewery wastewater (Driessen and
117 Vereijken, 2003). To simulate these compounds, yeast, malt, peptone, beer, acetic acid,
118 propionic acid and butyric acid were included in the recipe. Most of the ingredients are
119 fully soluble, except yeast and malt extract. From the total COD content per gram of
120 product, 70% of yeast's COD content is particulate and for malt extract, only 3%. So in
121 both, raw and fermented medium, around 90% of the particulate COD was provided by
122 the yeast. Regarding VFA concentration, reports from Palm Brewery ('personal
123 communication') showed that VFA corresponded to around 14% of the soluble COD in
124 the raw brewery wastewater. The COD from the VFA was divided between acetic acid
125 (40%), propionic acid (50%) and butyric acid (10%) (Ahn et al., 2001; Scampini, 2010).
126 To avoid any potential limitation of the AHB growth, nitrogen (N) and phosphorus (P)
127 both were dosed in excess. N and P target values were set by calculating maximum
128 biomass production assuming 100% COD removal efficiency, maximum observed yield

129 (Y_{obs}) of 1 g COD_{biomass}/g COD_{removed} (Meerburg et al., 2016) and a typical activated
130 sludge biomass composition C₅₀H₈₇O₂₃N₁₂P. A safety factor of +50% was included and
131 the final COD:N:P ratio was defined, 42.0:5.4:1.0. For other macronutrients, such as Ca,
132 Cl, Fe, Mg, Na, K and S, literature was used to define the recommended levels (Grady
133 Jr. et al., 2011). Micronutrients were not dosed assuming that tap water used in the
134 preparation of the media would contain the amount necessary for the microbial growth.
135 The fermented brewery wastewater was calculated based on the COD concentration of
136 the raw influent and literature data about the amount of COD lost and converted into
137 VFA during the fermentation process. Based on real wastewater fermentation
138 experiments performed by Ahn et al. (2001) and Alexiou (1998), it was assumed a
139 conversion ratio of 0.42 g VFA as COD/g total COD_{influent} and that 15% of the total
140 incoming COD would be lost because microbial growth was assumed. Thus, the VFA
141 concentration would correspond to 49% of the total COD in the fermented wastewater
142 and the same VFA speciation, as in raw wastewater, was used. Table 1 resumes all the
143 main target values used to formulate raw and fermented synthetic brewery wastewater.
144 It was decided to work with a 20 times concentrated medium. In this way, small
145 volumes could be kept in a fridge (4°C) during the tests, safeguarding media quality.
146 The concentrated medium was prepared every week. To prepare it, 2 L of demi water
147 was added to a 5 L recipient. Under thorough mixing by a magnetic stirrer, each
148 inorganic compounds was added per time till complete dissolution. Next, the organic
149 products were added one by one. After that pH was corrected to 7 using 2 M NaOH and
150 finally 1 mL of antifoam (SE-15, Sigma Aldrich) was added per liter of concentrated
151 medium. Finally, the demi water was added to the medium reaching a final volume of 5
152 L and then the effluent was stored at 4°C for usage. A 150L vessel containing tap water

153 and a 0.03M phosphate buffer solution was used to dilute the medium to the final
154 concentration and to keep the pH stable in the experiments. The buffer was the main
155 source of P for the bacteria. Information on brewery wastewater characteristics,
156 ingredients' composition and media recipe is provided ([see Supplementary Material](#)).

157 **2.2. Reactor setup and operation**

158 The main characteristics of the scenarios are shown in Table 2. Two 2 L acrylic
159 sequencing batch reactors (SBR) were operated simultaneously. One reactor was always
160 fed with synthetic raw wastewater while the other with synthetic fermented substrate.
161 Meanwhile, both reactors were kept at the same SRT (0.25, 0.50 or 1.00 d) and
162 operation mode (HiCAS or HiCS). Biomass was collected from a CAS plant treating
163 brewery wastewater from AB InBev (Leuven, Belgium) and stored at 4°C for
164 (re)inoculation whenever it was necessary to reach 1.5 g VSS/L. Concentrated medium
165 and tap water with buffer solution was added to reach 2 L volume and then the reactor
166 was started in batch mode for at least 1-2 d, then continuous operation was started. An
167 acclimation period of 3-5 days was respected, to reach steady-state, prior to resuming
168 sampling. Samples were taken daily.

169 The reactors were placed in a temperature-controlled room (20°C), and pH was kept
170 automatically at 7.00 ± 0.40 by a controller (Consort, Belgium). Overhead stirrer was
171 used for mixing, air pumps for aeration and peristaltic pumps controlled were used to
172 add influent (concentrated medium plus water), harvest biomass and remove the treated
173 effluent. Timers were used to set the exact time of equipment operation according to the
174 reactor phases. Total cycle time in both reactors was 120 min. For HiCAS the phases
175 were: feed and react (100 min aerated), settle (15 min), withdraw (4 min) and idle (1
176 min). In the HiCS system the cycle was divided as follows: feed and contact (28 min,

177 unaerated), stabilization (72 min, aerated), settle (15 min), withdraw (4 min) and idle (1
178 min). The contact to stabilization time ratio used was 0.38, the optimal found by
179 Meerburg et al. (2016). The harvesting of the biomass was performed during the react
180 phase in HiCAS and during the contact phase in HiCS.

181 **2.3. Analytical procedures**

182 Total suspended solids (TSS) and volatile suspended solids (VSS) were determined
183 according to standard methods (Greenberg et al., 1992) and used to quantify biomass in
184 the system. Photometric test kits (Merck, Germany) were used to measure COD
185 fractions, total (COD_t) and soluble (COD_s). Prior to COD_s determination, the sample
186 was filtered using a 0.2 µm syringe filter (Chromafil PTFE, Macherey-Nagel) to remove
187 particles. COD particulate (COD_p) was obtained by the difference between COD_t and
188 COD_s. Colloidal COD, represented by the solids with size between 0.20-25 µm, were
189 therefore deliberately accounted together with the COD_p and the fate of these particles
190 were not investigated although recommended for future studies.

191 Protein content was determined according to a modified Lowry method as described in
192 Markwell et al. (1978). The protein values were expressed as a fraction of total
193 suspended solids (TSS). Amino acid (AA) residuals measurements started with a
194 hydrolysis step, which was performed with 6M HCl for 24 hours at 110°C, in vacuum-
195 sealed hydrolysis tubes (Wilmad Labglas). To avoid AA oxidation, hydrolysis and
196 subsequent acid evaporation were performed under vacuum atmosphere, alternating
197 with nitrogen gas flushing. After evaporation and dissolution in 0.75 mM HCl, samples
198 were stored at -20°C. AA were derivatised with propyl chloroformate following the
199 EZ:faast kit amino acid analysis procedure (Phenomenex, 2003). Injection volume was
200 2 µL with a split ratio of 1:25 and the injection temperature of 250°C. Helium at a

201 constant flow of 1.1 mL/min was used as a carrier gas. The oven temperature was set to
202 increase 30 °C/min from 110 °C to 320 °C. The separation of the sample was done
203 using a using a Zebron TM EZ-AAA Amino Acid GC 10 m x 0.25 mm column
204 (Phenomenex) and the analyses were performed with gas chromatography mass
205 spectrometry (Agilent HP6890 Series GC system Plus; HP 5973 Mass selective
206 detector). The MSD Chemstation E.02.01.117 (Agilent Technologies. Inc., Santa Clara,
207 CA) software was used for the data analysis. Parallel analysis of Bovine Serum
208 Albumin (BSA) at a known concentration was performed to determine AA recovery.
209 Arginine was not measured, and tryptophan was destroyed during acid hydrolysis.
210 Essential amino acids (EAA) data were normalized by the rainbow trout's EAA
211 requirements in order to compare the scenarios.

212 **2.4. Calculations**

213 SRT was calculated as total biomass in the reactor divided by the sum of the daily
214 biomass harvested and the biomass present in the effluent, while Y_{obs} was calculated as
215 in Meerburg et al. (2015). COD mass balance was calculated for each scenario, using
216 the mean daily values obtained during steady state, in order to determine the fate of
217 COD during the process. The mass balance takes in consideration the influent COD, as
218 soluble ($COD_{s,inf}$) and particulate ($COD_{p,inf}$), and the outgoing COD fractions of the
219 particulate biomass harvested ($COD_{p,harv}$), and particulate and soluble effluent COD
220 ($COD_{p,eff}$ and $COD_{s,eff}$). The unaccounted COD, the portion that enters the process and
221 does not leave in the effluent, was assumed to be oxidized to CO_2 through microbial
222 respiration, here represented as $COD_{Oxidized}$. The sum of the outgoing particulate COD,
223 harvested and in the effluent, corresponds to the COD redirected, assuming that all
224 solids after the process are potential MP. COD removal efficiency was calculated as the

225 difference between the incoming total COD and soluble COD divided by the total COD
226 influent while COD removal rate was calculated using the formula:

$$227 \text{ COD}_{\text{removal rate}} = \text{Flow} \times (\text{total COD}_{\text{influent}} - \text{soluble COD}_{\text{effluent}}) / (0.83 \times \text{Reactor volume})$$

228 The factor 0.83 used in the COD removal rate is added to discount the settling time,
229 withdraw and idle, from the total reaction phase (i.e., contact, stabilization). The final

230 AHB product was considered as the sum of biomass harvested and present in the

231 effluent, expressed as TSS. The daily AHB biomass and protein volumetric

232 productivities were calculated as:

$$233 \text{ AHB productivity} = \text{Flow} \times (\text{TSS}_{\text{harvested}} + \text{TSS}_{\text{effluent}}) / \text{Reactor volume}$$

$$234 \text{ Protein productivity} = \text{AHB productivity} \times \text{AHB protein content} \%$$

235 **2.5. Microbial community analysis**

236 One sample per each different scenario was taken and stored at -20°C in order to
237 preserve the genetic material until further processing. Total DNA content extraction was

238 done using the Powerfecal kit (Qiagen, Germany) and following the manufacturers

239 protocol. The DNA extracts were sent to Novogene Biotech Co., Ltd (United Kingdom)

240 for amplicon sequencing analysis. Amplification of the V3-V4 hypervariable region of

241 the 16S rRNA was performed using the primers forward 341f

242 (CCTAYGGGRBGCASCAG) and reverse 806r (GGACTACNNGGGTATCTAAT)

243 and carried out with Phusion® High-Fidelity PCR Master Mix (New England Biolabs).

244 The amplicon sequencing libraries were pooled and sequenced in an Illumina paired-

245 end platform. After sequencing, the raw reads were quality filtered, chimeric sequences

246 were removed, and the amplicon sequence variants (ASVs) were obtained using

247 DADA2 (Callahan et al., 2016) and ASVs were classified using the EzTaxon database

248 (Chun et al., 2007). Downstream microbial community analysis was performed using

249 tidyamplicons (<https://github.com/SWittouck/tidyamplicons>) in the R (v.4.0.2) for
250 windows (R Core Team, 2020). Alpha and beta diversity were calculated using Inverse
251 Simpson and Bray-Curtis dissimilarity indices respectively. Principal Coordinate
252 Analysis (PCoA) was performed to visualize the dissimilarities between microbial
253 communities in the tested scenarios. Bray-Curtis distance between samples followed by
254 hierarchical average linkage clustering of samples was done. Then, Permutational
255 Multivariate Analysis of Variance (PERMANOVA), with number of permutations set to
256 999, was made to identify significant effect of the independent variables on the
257 microbial structure. The top 11 most common ASV, at phylum and genus level, were
258 plotted in a stacked bar graph. The raw data generated from 16S rRNA gene
259 sequencing is available at the European nucleotide archive (<https://www.ebi.ac.uk/>) via
260 the accession number: PRJEB55306.

261 **2.6. Statistical analyses**

262 Normality of data residuals was tested using the Shapiro–Wilk test and homogeneity of
263 variances using Levene’s test. In case the null hypothesis of normality was accepted,
264 multiple comparisons were performed using analysis of variance (ANOVA) test and
265 post-hoc pairwise comparison Student’s *t*-test. In case of unequal variances, Welch’s
266 correction for ANOVA was applied followed by a Games-Howell pairwise comparison.
267 If normality was rejected, the non-parametric Kruskal–Wallis rank sum test and a post-
268 hoc pairwise Wilcoxon Rank Sum test was performed. Pairwise comparisons were just
269 used in case the null hypothesis of equal means was rejected and *p*-values were
270 corrected using the Bonferroni method. Significant differences were considered for *p*-
271 values below 0.05. Multiple linear regression (MLR) was done using a stepwise
272 backwards modelling strategy starting with the full model containing all three

273 independent variables (substrate, reactor and SRT), all pairwise interactions and the
274 triple interaction term. The main dependent variables of interest were included in the
275 model. This model was simplified by removing the least significant term, based upon
276 the p -value, starting with the highest order terms. Cut-off for significance was 0.01 to
277 account for multiple hypothesis testing and to reduce the chance of type I error (see
278 **Supplementary Material**). All statistical tests were performed with the software R
279 (v.4.0.2) for Windows (R Core Team, 2020).

280 **3. Results and discussion**

281 **3.1. COD redirection and observed yield**

282 The process applied needs to work concomitantly as a AHB production system and
283 wastewater treatment. Redirecting COD from the liquid stream to the MP final product
284 is the preferred COD removal pathway, thus minimizing COD oxidation to CO₂ is
285 desired. The remaining suspended and soluble COD in the treated effluent should be
286 reduced if possible as they represent biomass and substrate losses respectively. To
287 reveal the COD fate for each scenario, a COD mass balance was calculated using the
288 mean daily values during steady state conditions (Fig.1) and values are presented as a
289 percentage of the total COD influent.

290 Type of reactor had a more evident impact on COD_{p,harv} and COD redirection (the sum
291 of COD_{p,harv} and COD_{p,eff}) than type of substrate and SRT (Fig.1). MLR showed that the
292 type of reactor alone ($p = 1.08E-12$) and the interaction of medium with SRT ($p =$
293 $8.64E-4$) had a significant effect in the COD redirection. HiCAS' values for redirection
294 ranged between 46-72% while HiCS' remained between 40-47%, with overall means of
295 60% and 45% respectively. The highest COD redirection was obtained in HiCAS
296 reactor treating raw substrate under SRT of 0.50 d (72%) and 1.00 d (70%). These COD

297 redirection values are comparable to the results in other HRAS studies on domestic
298 wastewater (Jimenez et al., 2015; Meerburg et al., 2015; Rahman et al., 2016), equaling
299 the highest redirection value (72%) obtained by Rahman et al. (2019). Per SRT, the
300 ranges for COD redirection means for 0.25 d, 0.50 d and 1.00 d were respectively 40-
301 59%, 47-72%, 44-70%. Within the same type of substrate and reactor, processes at SRT
302 0.50 d had always higher COD redirection than SRT 1.00 d while both had superior
303 values than SRT 0.25d. The same trend was found for COD_{harv}. Thus, in this study,
304 among the SRTs tested, scenarios using SRT 0.50d can be considered the best for COD
305 redirection and harvesting. The highlight was the HiCAS reactor at raw substrate and
306 SRT 0.50 d that reached 71% of COD_{harv} with an extremely low COD particulate
307 fraction ending in the effluent (1%). Considering that 10% of the total influent COD is
308 particulate, and that 90% of the COD_p comes from the yeast added to the media, it is
309 possible that this product would be completely or partially hydrolysed, or end up in the
310 final AHB product. Assuming that all COD_p would form part of the final biomass, this
311 would represent 12-26% of the total COD harvested at maximum. As both ingredients
312 are feed grade, the potential presence of these compounds in the final product is not a
313 problem, in fact, it might contribute to its quality as spent yeast is typically used as feed
314 for animals. Understanding the impact of yeast on the final MP product is out of the
315 scope in this research, thus, further investigation would be necessary.

316 Regarding the particulate COD in the effluent, most of the reactors obtained below 7%
317 with an average value of 5%. The only exception to this range was found in the
318 condition raw, HiCAS, SRT 1.00 d, where the mean particulate COD losses was 17%.

319 Thus, in almost all the tested cases, most of the redirected COD is harvested indicating a
320 satisfactory bioflocculation process favouring settling. Interestingly, good settleability is

321 often a problem in HRAS systems treating low-strength wastewater (Rahman et al.,
322 2016) where COD_p losses to the effluent can go up to 54% (Meerburg et al., 2015).
323 Nevertheless, care should be taken when comparing these results as several factor can
324 affect the bioflocculation, and therefore settleability, such as the type of reactor
325 operation (i.e. SBR, plug-flow, HiCS, HiCAS), specific-loading rate, shear force, etc.
326 (Meerburg et al., 2015; Rahman et al., 2019). MLR pointed to a triple interaction
327 between substrate, reactor and SRT causing a significant impact on COD_{p,eff} ($p = 7.2E-$
328 7 , $R^2 = 62\%$) showing the complexity of this process. The most noticeable differences
329 between the literature and this study, are the strength and composition of the substrate,
330 and the substrate fill time. It is known that the influent composition affect microbial
331 growth (Fatemeh et al., 2019) thus it can have an impact on the microbial community,
332 floc structure and settleability. Hence it can be expected that studies using different
333 substrates could lead to a distinct biomass settling behavior. Moreover, the quick and
334 intermittent feeding regime in the SBR, lasting only 5 min per cycle, favours the
335 formation of a large COD gradient between the beginning (high COD level) and end of
336 the cycle (low COD level). The presence of a pronounced substrate gradient, due to the
337 short fill time, can have a strong positive effect on biomass settleability (Martins et al.,
338 2003). Although these two factors may have contributed to the low biomass presence in
339 the effluent in this study, the precise mechanisms are unknown.

340 Lower SRT typically results in a higher soluble COD fraction in the effluent and lower
341 fraction of COD oxidized (Meerburg et al., 2015). HiCAS clearly obtained lower CODs
342 results, between 2-41% than HiCS, 24-44%. Both trends can be seen in most of the
343 cases (Fig.1) within the same reactor and substrate. MLR confirms that CODs results
344 were significantly affected by the interaction between reactor and SRT ($p = 4.3E-5$, $R^2 =$

345 74%) while $COD_{Oxidized}$ was influenced by SRT ($p = 2.6E-6$) and by the interaction
346 between substrate and reactor ($p = 7.2E-3$). When comparing the $COD_{Oxidized}$ at the
347 same reactor and SRT, raw wastewater had always lower values than fermented. This
348 indicates that different types of substrates could lead to different COD oxidation levels
349 and recovery. HiCS had always higher CODs and lower $COD_{Oxidized}$ meaning that an
350 important fraction of the substrate was not oxidized to CO_2 due to the absence of oxygen
351 in the contact phase which prevented the growth of the aerobic bacteria. Keeping the
352 contact phase unaerated was a strategy selected to promote the biosorption (Meerburg et
353 al., 2015), which is an important route for organic matter capture and to increase the
354 observed yield of the biomass. Rahman et al. (2019) managed to obtain microbial
355 growth and biosorption by maintaining a low concentration of oxygen (around 0.5 mg
356 O_2/L) in the contact phase and this approach is suggested for future investigations.
357 Statistical analysis did not find any difference between the Y_{obs} , probably due to the
358 high variation of the data. The values remained between 0.56-0.81 $g\ COD_{biomass}/g$
359 $COD_{removed}$ for HiCAS and 0.64-0.78 $g\ COD_{biomass}/g\ COD_{removed}$ for HiCS. The obtained
360 results indicate that a timid biosorption may have occurred in the scenarios where Y_{obs}
361 were above the maximum theoretical biological yield of 0.4-0.7 $g\ COD/g\ COD_{removed}$ for
362 heterotrophic growth (Metcalf & Eddy, 1991), knowing that HRAS systems can reach
363 up to 1 $g\ COD/g\ COD_{removed}$ (Meerburg et al., 2016). Still, the results are considered
364 satisfactory for carbon recovery, specially under raw substrate processed by HiCAS in
365 SRT between 0.5-1.0 d, where high yields (0.76-0.77 $g\ COD/g\ COD_{removed}$) and COD
366 redirection (70-72 %) were obtained. Therefore, based on all the results above, it is
367 possible to affirm that HiCAS had a better performance than HiCS, due to its higher
368 COD redirection and harvesting and lower CODs in the effluent.

369 3.2. COD removal rate and efficiency

370 The COD removal rate and efficiency determines the performance of the tested
371 conditions in the wastewater treatment perspective (Fig. 2). The reactors at SRT of 0.50
372 d had the highest COD removal rate, up to 16 g COD/L_{reactor}/d in HiCAS and HiCS
373 reactors at raw substrate. COD removal rates were always lower at SRT 0.25 d. At such
374 a low SRT, high specific loading rate are applied causing deterioration of the COD
375 removal but typically can bring the advantage of obtaining higher observed yield
376 (Vriens et al., 1989), thus increasing the efficiency of carbon capture. As mentioned
377 above, Y_{obs} did not differ significantly between SRTs, thus the 0.25 d SRT did not pose
378 an advantage to the process. Next, at the same substrate and reactor type, the mean COD
379 removal rate at SRT 0.50 was 13-19% higher than at SRT 1.00. This difference was not
380 statistically significant in almost all the cases, except at raw and HiCAS, but this was
381 caused by the lower COD loading rate applied in these reactors in order to keep the
382 biomass in levels in which the sludge blanket could settle and compress thus avoiding
383 significant losses as COD_p in the effluent.

384 HiCAS reactors obtained high removal efficiencies, both with raw substrate (98% for
385 HiCAS SRT 0.50 d and 94% for HiCAS SRT 1.00 d), as well as fermented (97% for
386 HiCAS SRT 0.5 and 96% for HiCAS SRT 1.00 d). In fact, it is known that low SRT
387 (below 2 d) is sufficient to allow a substantial removal of soluble COD (Grady Jr. et al.,
388 2011). Brewery wastewater typically contains high fractions of readily degradable
389 organics, thus, high removal efficiencies can be expected even at a low SRT. The lower
390 COD removal efficiency in HiCS reactors, between 56-75%, and the reasons were
391 discussed in the previous section. Thus, results show that HiCAS reactors operating at
392 0.50 d was the optimal strategy to reach high COD removal rates and efficiencies.

393 3.3. AHB protein content and productivities

394 From the MP production perspective, reaching high protein content is a desirable
395 feature. In Fig.3A, it is possible to verify that AHB's mean protein content among all
396 the tested scenarios remained between 37.0-47.5% on dry weight, which is within the
397 interval found in literature. Vriens et al. (1989) found protein levels ranging between
398 30-50% (dry weight basis). Muys et al. (2020) sampled AHB biomass from 25
399 companies from the food and beverage industry obtaining a protein levels between 21-
400 49 % on dry weight. Protein levels within the same type of substrate were statistically
401 similar, independent of the type of reactor and SRT. MLR analysis showed that only the
402 substrate had a significant effect on protein levels ($p = 5.1E-5$). The mean protein
403 content obtained in the reactors fed with raw and fermented wastewater were 39% and
404 45% on dry weight, respectively. Thus, there is an absolute mean difference of 6% that
405 is incremented to the protein level of AHB biomass produced on fermented wastewater.
406 In fact, Dohanyos et al. (1978) showed that the type of influent composition had an
407 impact on AHB's protein level but there is still a lack of information about the effect of
408 complex substrate matrix to the MP biomass quality and it poses an opportunity to
409 increase protein productivity requiring further investigation. Other factors were
410 suggested to influence AHB protein levels such as SRT, COD/N ratio, COD/P ratio, N-
411 specific loading rate and pH (Muys et al., 2020; Vriens et al., 1989). From these, only
412 SRT could had caused an effect in protein levels as pH was kept stable at 7.00 using a
413 controller, nutrients (N and P) were dosed in excess and COD:N:P ratios were the same
414 in both substrates. COD:N:P was kept the same in both substrates to avoid confounding
415 factors that could hamper the results. Thus if substrate would cause a significant effect
416 to the dependent variables (i.e., biomass productivity, protein level), this can be only

417 explained by the difference in COD level and fractionation (i.e. presence of VFA). The
418 effect of SRT on the protein level was not detected likely due to low and narrow range
419 (0.25-1.00 d) applied compared with other studies, 2-66 d (Muys et al., 2020; Tucek et
420 al., 1977), where a negative relation between SRT and protein content was found.

421 MLR showed that AHB and protein productivity were affected significantly by type of
422 substrate in combination with SRT levels. Biomass productivity (Fig.3B) was higher in
423 reactors operated under raw wastewater (6.14-7.97 g TSS/L/d) compared with the ones
424 under fermented substrate (4.37-6.92 g TSS/L/d). When comparing the same type of
425 reactor and SRT between raw and fermented scenarios, the mean biomass productivity
426 was higher in reactors processing raw wastewater in almost all the cases, except for
427 HiCAS at SRT 0.25 d. However, the higher protein level for scenarios using fermented
428 substrate raised protein productivities to levels equivalent to those obtained under raw
429 wastewater. The maximum biomass and protein productivity was attained in HiCAS
430 reactor fed with raw wastewater at SRT of 0.50 d, respectively 7.97 g TSS/L/d and 2.95
431 g protein/L/d, followed by HiCAS under fermented wastewater at SRT of 0.25 d
432 reaching biomass and protein production of 6.92 g TSS/L/d and 3.21 g protein/L/d,
433 respectively. Results show that protein productivities were typically lower at SRT 1.00
434 d, compared to 0.25 and 0.50 d. The best productivity was achieved at SRT 0.50 d,
435 making this the preferred operational setpoint.

436 Fermented substrate had a positive impact on protein levels and productivity.

437 Nevertheless, the inclusion of an anaerobic fermentation step would increase the
438 complexity of the production process as this extra biological step would require
439 additional operational care to guarantee stable fermentation conditions and substrate
440 quality for the aerobic process. This would, consequently, reduce variabilities to the

441 AHB biomass production. Although it would result in an additional operational burden,
442 similar protein productivities can be achieved with 13% less biomass, difference found
443 when comparing the highest AHB productivity using raw substrate versus the highest
444 productivity using fermented (Fig. 3B). This means a lower demand for the downstream
445 processing which represents by far the highest operation costs in MP production (Spiller
446 et al., 2020) thus the economics remain to be evaluated. Compared to other MP, AHB
447 outperformed PNSB and MaB. Alloul et al. (2019) obtained a PNSB productivity of 1.7
448 g DW/L/d (46% protein content), the maximum reported for this bacteria. The
449 maximum MaB productivity reached by Van Den Hende (2019) was 0.26 g DW/L/d
450 (28% protein level).

451 In this study, the best overall scenario was operated with raw brewery wastewater,
452 HiCAS reactor and SRT 0.50 d. This scenario obtained the highest mean COD
453 redirection and harvesting with the lowest effluent soluble and particulate COD, while
454 the protein levels and observed yield did not differ substantially among the 12 tested
455 treatments. Raw substrate has higher potential based on its COD redirection with lower
456 COD oxidation, however, it did lead to poorer soluble and particulate COD effluent.
457 Further research into solids separation is therefore needed. Fermented effluent had a
458 statistically higher protein level content, thus a trade-off between redirection and
459 specific protein production is apparent. Further investigation is consequently necessary.

460 **3.4. AHB essential amino acids profile**

461 The EAAs cannot be synthesized by the target organism and therefore need to be
462 obtained through the diet. Here, rainbow trout was chosen as the target organism as
463 salmonids are the largest consumers of FM , 15% of the total FM used in aquaculture in
464 2019 (EUMOFA, 2021), and have the biggest share in value of the global fish market

465 since 2013 (FAO, 2020). For salmonids there are ten EAA and eight of them were
466 measured: histidine, isoleucine, leucine, lysine, methionine + cysteine (met+cys),
467 phenylalanine + tyrosine, threonine, and valine. In Fig.4, the EAA composition of the
468 AHB, from the 12 scenarios tested, and FM (Heuzé et al., 2015) were normalized to the
469 EAA requirements of rainbow trout (Ogino, 1980). All scenarios yielded an AHB
470 biomass with an outstanding EAA profile, comparable to FM, and matching rainbow
471 trout requirements. Only the levels of the sulphur-containing EAA (met+cys) were
472 deficient in all scenarios reaching a mean value of $25\pm 22\%$ of rainbow trout's
473 requirement although a broad range was found, from 1.7 to 22.5 mg (met+cys)/g of
474 protein. The coefficient of variance of the others EAA amongst all the scenarios
475 remained between 12-26%, way lower compared to the sulphur-containing EAA (86%).
476 Muys et al. (2020) investigated the AHB biomass quality of conventional activated
477 sludge from 25 different food industries and also found that methionine + cysteine were
478 the EAA with highest variability with values ranging between 0.3-28 mg (met+cys)/g of
479 protein which are quite similar to the ones obtained in this study. These EAAs are
480 known to be limiting in AHB biomass and other microorganisms (Vriens et al., 1989).
481 Currently, one way of dealing with this problem is to blend AHB biomass to
482 methionine-rich products or to add synthetic methionine. In both cases, economic and
483 sustainable issues need to be taken in consideration. Overall, reactors treating raw
484 wastewater had a total EAA value between 361-534 mg EAA/g of protein while
485 fermented had 300-434 mg EAA/g of protein, thus raw reactors were on average 18%
486 higher than fermented. This fact, together with the high variability of individual EAA,
487 indicate a potential to steer amino acid profile by changing operational conditions and
488 should be further investigated.

489 **3.5. Microbial community**

490 Revealing the predominant composition of the microbial community and understanding
491 how the different operational conditions affect it is essential for the process
492 development. As most of the operational parameters were controlled just substrate, type
493 of HRAS and SRT could influence the AHB community. PCoA analysis on the Bray-
494 Curtis distance matrix (Fig. 5) showed the similarities between the bacterial community
495 composition at genus level for each of the tested scenarios. Samples ordinated closer to
496 one another are more similar regarding their bacterial community structure than those
497 that are more distant. Three clusters could be observed: i) cluster 1 was formed by all
498 the four scenarios testing SRT 0.25 d plus the fermented HiCS 1.00 d sample; ii) cluster
499 2 was formed by all the four samples operated at SRT 0.50 d plus the raw HiCS 1.00 d
500 sample; iii) cluster 3 was represented by the two HiCAS reactor at SRT 1.00 d samples,
501 under raw and fermented substrate. PERMANOVA analysis confirmed that only SRT
502 had a significant influence ($p = 2.2E-2$) over the AHB bacterial community in our set-
503 up. Strong correlations between SRT and microbial community changes were
504 previously reported in both high and low-rate AS (Gonzalez-Martinez et al., 2016;
505 Valentín-Vargas et al., 2012). HiCS at SRT 1.00 d under fermented (cluster 1) and raw
506 substrate (cluster 2) did not group with their correspondent SRT (cluster 3) as it would
507 be expected. These two strayed scenarios were operated in the same period, in parallel,
508 and had the same inoculum. Nevertheless, laboratory-scale reactors operated under
509 similar conditions had no reproducibility in the microbial community and shifts
510 occurred over time in Boon et al. (2000). Chance-driven processes could force the
511 bacterial community to evolve differently to similar perturbations (Kaewpipat and

512 Grady, 2002). This effect is to be more pronounced in small-scale reactors (Curtis et al.,
513 2003), and therefore could have happened in this study.

514 Alpha-diversity and relative abundances were also obtained (see Supplementary
515 material). Studies pointed that lower SRT leads to lower diversity (Gonzalez-Martinez
516 et al., 2016; Meerburg et al., 2016). Here, alpha-diversity did not follow a clear trend
517 based on any parameter although scenarios using raw substrate had typically a higher
518 Inverse Simpson index. The Inverse Simpson (richness and evenness) and observed
519 species (richness) for all the scenarios remained between 3-33 (mean = 11) and 404-957
520 (mean = 571) respectively. The limited number of samples and the short range of SRT
521 (0.25-1.0 d) are a potential bias to these results. Taxonomic assignment of ASV
522 identified 47 phyla among all the scenarios while just 10 were present in all the
523 samples. The relative abundance of the top three dominant phyla were varying between
524 20-81% for Proteobacteria (mean = 60%), 5-73% for Bacteroidetes (mean = 25%) and
525 1-44% for Firmicutes (mean = 8%). Together these phyla represented between 78-98%
526 (mean = 93%) of the total reads. Proteobacteria and Bacteroidetes are by far the most
527 common phylum in high and low rate AS (Gonzalez-Martinez et al., 2016; Meerburg et
528 al., 2016). In total, 923 genera were found only 23 were present in all the tested
529 scenarios. The relative abundance of the top 11 genera remained between 48 and 82%
530 (mean = 66%) of the total counts comprising strictly and facultative aerobic organisms.
531 Some genera such as *Acinetobacter*, *Arcobacter* and *Leadbetterella*, obtained a relative
532 abundance close or higher than 50% in at least one scenario.

533 **4. Conclusions**

- 534 • HiCAS and the novel HiCS can achieve high AHB and protein productivities, along
535 with great EAA profiles.

- 536 • High observed yields and outstanding COD removal were obtained in HiCAS.
- 537 • The best performance was obtained using raw substrate, HiCAS and SRT 0.50 d.
- 538 • More studies in AHB community and biomass quality steerability are essential.
- 539 • Necessity to evaluate process techno-economic feasibility.
- 540 • HRAS can be the key process to turn AHB MP product into reality.

541 **Declaration of competing interest**

542 None.

543 **Acknowledgements**

544 The authors kindly acknowledge the Research Foundation Flanders (FWO-Vlaanderen)
545 for supporting G.P. with a doctoral fellowship (strategic basic research: 1S38917N).
546 Special thanks to AB InBEV NV, Duvel Moortgat NV and Palm Breweries NV for
547 providing samples to this work. Graphical abstract used images from Freepik.com.

548 **References**

- 549 1. Ahn, Y.H., Min, K.S., Speece, R.E., 2001. Pre-acidification in anaerobic sludge bed
550 process treating brewery wastewater. *Water Res.* 35, 4267–4276.
- 551 2. Alexiou, I.E., 1998. A study of Pre-Acidification Reactor Design for Anaerobic
552 Treatment of High Strength Industrial Wastewater. Newcastle University.
- 553 3. Alloul, A., Wuyts, S., Lebeer, S., Vlaeminck, S.E., 2019. Volatile fatty acids
554 impacting phototrophic growth kinetics of purple bacteria: Paving the way for protein
555 production on fermented wastewater. *Water Res.* 152, 138–147.
- 556 4. Boon, N., Goris, J., De Vos, P., Verstraete, W., Top, E.M., 2000. Bioaugmentation of
557 activated sludge by an indigenous 3-chloroaniline- degrading *Comamonas testosteroni*
558 strain, I2gfp. *Appl. Environ. Microbiol.* 66, 2906–2913.

- 559 5. Callahan, B.J., McMurdie, P.J., Rosen, M.J., Han, A.W., Johnson, A.J.A., Holmes,
560 S.P., 2016. DADA2: High-resolution sample inference from Illumina amplicon data.
561 Nat. Methods 2016 137 13, 581–583.
- 562 6. Chun, J., Lee, J.H., Jung, Y., Kim, M., Kim, S., Kim, B.K., Lim, Y.W., 2007.
563 EzTaxon: a web-based tool for the identification of prokaryotes based on 16S
564 ribosomal RNA gene sequences. *Int. J. Syst. Evol. Microbiol.* 57, 2259–2261.
- 565 7. Curtis, T.P., Head, I.M., Graham, D.W., 2003. Theoretical ecology for engineering
566 biology. *Environ. Sci. Technol.* 37, 64A-70A.
- 567 8. Dohanyos, M., Chudoba, J., Tucek, F., Grau, P., 1978. The influence of substrate and
568 micronutrients on formation of protein in activated sludge. *Tech. Res. Rep.*
- 569 9. Driessen, W., Vereijken, T., 2003. Recent developments in biological treatment of
570 brewery effluent. *Inst. Guild Brew. Conv. Livingstone, Zambia, March 2-7* 10.
- 571 10. Eddy, M.&, 1991. *Wastewater engineering: treatment, disposal and reuse*, 3rd ed.
572 McGraw-Hill, New York.
- 573 11. EUMOFA, 2021. *Fishmeal and fish oil: production and trade flows in the EU*.
574 Publications Office of the European Union, Luxembourg.
- 575 12. FAO, 2020. *The State of World Fisheries and Aquaculture - Sustainability in Action*.
576 Food and Agriculture Organization of the United Nations.
- 577 13. Fatemeh, S., Reihani, S., Khosravi-Darani, K., 2019. Influencing factors on single-cell
578 protein production by submerged fermentation: A review. *Electron. J. Biotechnol.* 37,
579 34–40.
- 580 14. Godfray, H.C.J., Beddington, J.R., Crute, I.R., Haddad, L., Lawrence, D., Muir, J.F.,
581 Pretty, J., Robinson, S., Thomas, S.M., Toulmin, C., 2010. Food security: The
582 challenge of feeding 9 billion people. *Science* (80-.). 327, 812–818.

- 583 15. Gonzalez-Martinez, A., Rodriguez-Sanchez, A., Lotti, T., Garcia-Ruiz, M.J., Osorio,
584 F., Gonzalez-Lopez, J., Van Loosdrecht, M.C.M., 2016. Comparison of bacterial
585 communities of conventional and A-stage activated sludge systems. *Sci. Reports* 2016
586 61 6, 1–11.
- 587 16. Grady Jr., C.P.L., Daigger, G.T., Love, N.G., Filipe, C.D.M., 2011. *Biological*
588 *Wastewater Treatment*, 3rd ed. CRC Press; IWA Publishing.
- 589 17. Heuzé, V., Tran, G., Kaushik, S., 2015. Fish meal. *Feedipedia*, a programme by INRA,
590 CIRAD, AFZ and FAO [WWW Document].
- 591 18. Kaewpipat, K., Grady, C.P.L., 2002. Microbial population dynamics in laboratory-
592 scale activated sludge reactors. *Water Sci. Technol.* 46, 19–27.
- 593 19. Markwell, M.A.K., Haas, S.M., Bieber, L.L., Tolbert, N.E., 1978. A modification of
594 the Lowry procedure to simplify protein determination in membrane and lipoprotein
595 samples. *Anal. Biochem.* 87, 206–210.
- 596 20. Martins, A.M.P., Heijnen, J.J., Van Loosdrecht, M.C.M., 2003. Effect of feeding
597 pattern and storage on the sludge settleability under aerobic conditions. *Water Res.* 37,
598 2555–2570.
- 599 21. Meerburg, F., Boon, N., Van Winckel, T., Vercamer, J., Nopens, I., Vlaeminck, S.,
600 2015. Toward energy-neutral wastewater treatment: A high-rate contact stabilization
601 process to maximally recover sewage organics. *Bioresour. Technol.* 179, 373–381.
- 602 22. Meerburg, F., Vlaeminck, S.E., Roume, H., Seuntjens, D., Pieper, D.H., Jauregui, R.,
603 Vilchez-Vargas, R., Boon, N., 2016. High-rate activated sludge communities have a
604 distinctly different structure compared to low-rate sludge communities, and are less
605 sensitive towards environmental and operational variables. *Water Res.* 100, 137–145.
- 606 23. Meerburg, F.A., Boon, N., Van Winckel, T., Pauwels, K.T.G., Vlaeminck, S.E., 2016.

607 Live fast, die young: Optimizing retention times in high-rate contact stabilization for
608 maximal recovery of organics from wastewater. *Environ. Sci. Technol.* 50, 9781–
609 9790.

610 24. Muys, M., Papini, G., Spiller, M., Sakarika, M., Schwaiger, B., Lesueur, C., Vermeir,
611 P., Vlaeminck, S.E., 2020. Dried aerobic heterotrophic bacteria from treatment of food
612 and beverage effluents: Screening of correlations between operation parameters and
613 microbial protein quality. *Bioresour. Technol.* 307, 123242.

614 25. Ogino, C., 1980. Requirements of Carp and Rainbow Trout for Essential Amino
615 Acids. *Nippon SUISAN GAKKAISHI* 46, 171–174.

616 26. Okoli, C.S., Okonkwo, P.C., 2016. Fluidized- Fluidized - Bed Reactor for Treatment
617 of Brewery Wastewater 35, 91–96.

618 27. R Core Team, 2020. A language and environment for statistical computing.

619 28. Rahman, A., De Clippeleir, H., Thomas, W., Jimenez, J.A., Wett, B., Al-Omari, A.,
620 Murthy, S., Riffat, R., Bott, C., 2019. A-stage and high-rate contact-stabilization
621 performance comparison for carbon and nutrient redirection from high-strength
622 municipal wastewater. *Chem. Eng. J.* 357, 737–749.

623 29. Rahman, A., Meerburg, F.A., Ravadagundhi, S., Wett, B., Jimenez, J., Bott, C., Al-
624 Omari, A., Riffat, R., Murthy, S., De Clippeleir, H., 2016. Bioflocculation
625 management through high-rate contact-stabilization: A promising technology to
626 recover organic carbon from low-strength wastewater. *Water Res.* 104, 485–496.

627 30. Rana, K.J., Siriwardena, S., Hasan, M.R., 2009. Impact of rising feed ingredient prices
628 on aquafeeds and aquaculture production, *FAO Fisheries and Aquaculture Technical*
629 *Paper*.

630 31. Ritala, A., Häkkinen, S.T., Toivari, M., Wiebe, M.G., 2017. Single cell protein-state-

631 of-the-art, industrial landscape and patents 2001-2016. *Front. Microbiol.* 8, 2009.

632 32. Scampini, A.C., 2010. Upflow anaerobic sludge blanket reactors for treatment of
633 wastewater from the brewery industry. Massachusetts Institute of Technology.

634 33. Spiller, M., Muys, M., Papini, G., Sakarika, M., Buyle, M., Vlaeminck, S.E., 2020.
635 Environmental impact of microbial protein from potato wastewater as feed ingredient:
636 Comparative consequential life cycle assessment of three production systems and
637 soybean meal. *Water Res.* 171, 115406.

638 34. Tucek, F., Chuboda, J., Dohanyos, M., Grau, P., 1977. The influence of sludge age on
639 formation of protein in activated sludge. *Prague Inst. Chem. Tech. Res. Rep.*

640 35. United Nations, Department of Economic and Social Affairs, P.D., 2019. World
641 Population Prospects 2019: Press Release.

642 36. Valentín-Vargas, A., Toro-Labrador, G., Massol-Deyá, A.A., 2012. Bacterial
643 community dynamics in full-scale activated sludge bioreactors: Operational and
644 ecological factors driving community assembly and performance. *PLoS One* 7.

645 37. Van Den Hende, S., 2014. Microalgal bacterial flocs for wastewater treatment: from
646 concept to pilot scale.

647 38. Van Winckel, T., Liu, X., Vlaeminck, S.E., Takács, I., Al-Omari, A., Sturm, B.,
648 Kjellerup, B. V., Murthy, S.N., De Clippeleir, H., 2019. Overcoming floc formation
649 limitations in high-rate activated sludge systems. *Chemosphere* 215, 342–352.

650 39. Verstraete, W., Clauwaert, P., Vlaeminck, S.E., 2016. Used water and nutrients:
651 Recovery perspectives in a “panta rhei” context. *Bioresour. Technol.* 215, 199–208.

652 40. Vriens, L., Nihoul, R., Verachtert, H., 1989. Activated Sludges as Animal Feed : A
653 Review 27, 161–207.

654

655 Table 1. Characteristics of the synthetic raw and fermented brewery wastewater

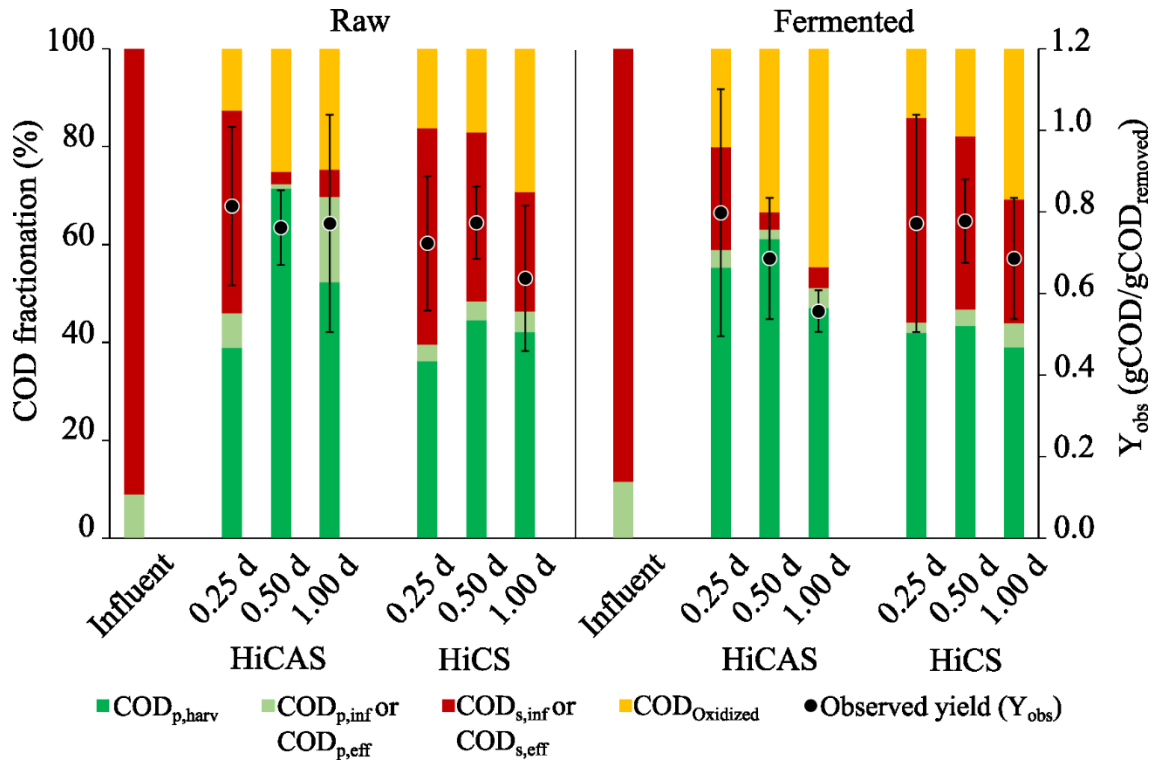
Parameter	Raw (g/L)	Fermented (g/L)
COD _{total}	3.700	3.145
COD _{particulate}	0.369	0.350
COD _{soluble}	3.331	2.795
COD _{soluble as VFA}	0.473	1.554
COD _{soluble as non-VFA}	2.858	1.241
BOD ₅	2.442	2.076
Total nitrogen, as N	0.478	0.406
Total phosphorus, as P	0.088	0.075

656

657 Table 2. Overview of reactor operation characteristics, biomass concentration and COD
 658 influent. SLR: specific loading rate; VER: volume exchange ratio

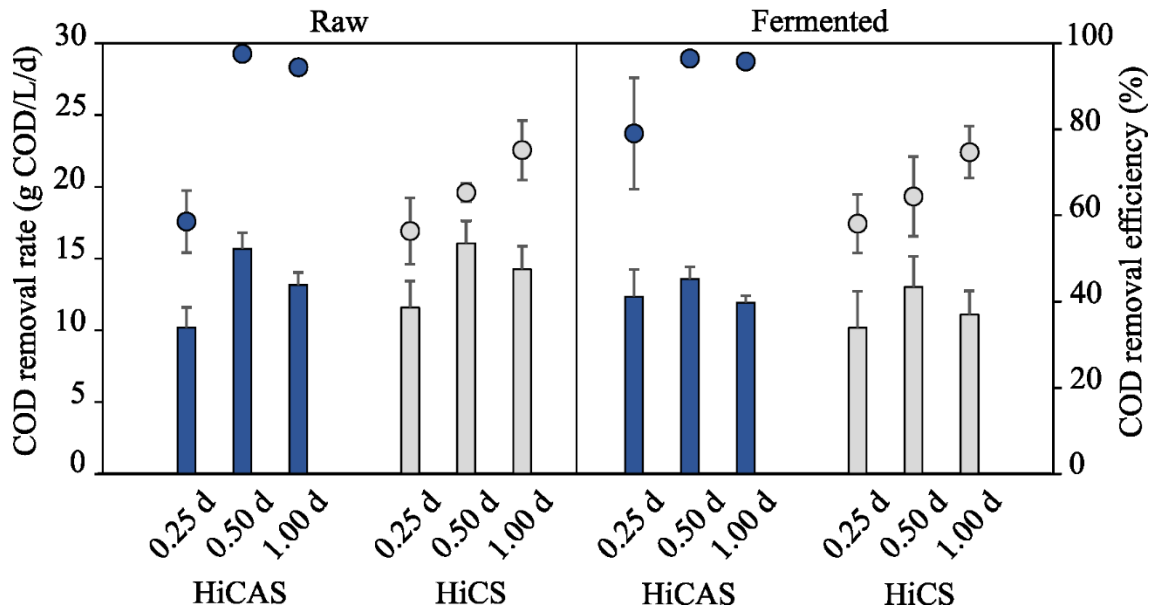
Substrate	Reactor	SRT d	SLR g COD _T /g VSS/d	COD _{influent} g COD _T /L	VER %	VSS g/L	VSS/TSS %
Raw	HiCAS	0.22 ± 0.01	13.1 ± 1.2	2.76 ± 0.16	44 ± 0	1.39 ± 0.18	87 ± 3
		0.50 ± 0.02	4.5 ± 0.4	3.67 ± 0.38	30 ± 1	3.48 ± 0.35	90 ± 2
		0.87 ± 0.12	2.7 ± 0.4	3.52 ± 0.24	27 ± 1	5.30 ± 0.60	86 ± 3
	HiCS	0.23 ± 0.01	14.4 ± 1.8	3.13 ± 0.36	46 ± 2	1.54 ± 0.36	91 ± 3
		0.49 ± 0.03	7.4 ± 1.1	3.55 ± 0.28	48 ± 2	3.32 ± 0.44	87 ± 5
		1.12 ± 0.07	2.9 ± 1.0	3.67 ± 0.41	36 ± 6	6.09 ± 0.67	89 ± 3
Fermented	HiCAS	0.24 ± 0.01	11.2 ± 2.3	2.59 ± 0.10	42 ± 0	1.35 ± 0.38	87 ± 5
		0.50 ± 0.02	5.3 ± 0.8	3.16 ± 0.30	31 ± 1	2.67 ± 0.24	88 ± 3
		1.17 ± 0.1	2.7 ± 0.3	3.17 ± 0.13	27 ± 1	4.68 ± 0.33	85 ± 3
	HiCS	0.24 ± 0.01	14.1 ± 3.4	2.67 ± 0.39	44 ± 1	1.33 ± 0.27	87 ± 4
		0.48 ± 0.03	7.5 ± 1.8	3.04 ± 0.33	46 ± 2	2.78 ± 0.61	88 ± 4
		1.09 ± 0.13	3.6 ± 0.9	2.75 ± 0.94	35 ± 5	4.21 ± 0.55	88 ± 5

659



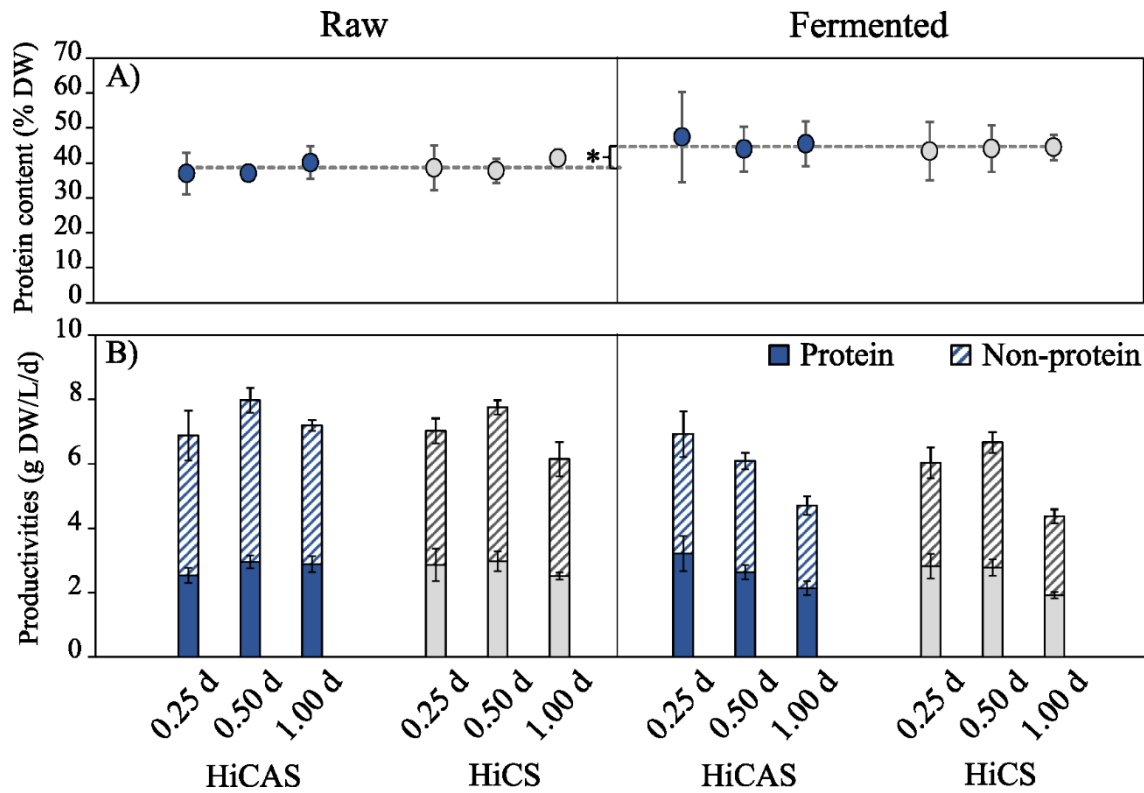
660

661 Fig.1. Fate of COD and observed yield (Y_{obs}) in the different scenarios based in the
 662 mean values obtained in a daily mass balance. Subscript “p” and “s” stands to
 663 particulate and soluble respectively, while “harv” represents the harvested fraction of
 664 the biomass, “inf” COD influent, and “eff” COD effluent of the process. Error bars
 665 correspond to the 95% confidence interval.



666

667 Fig.2. COD removal rate (bars) and efficiency (dots) in the 12 tested scenarios. HiCAS
 668 and HiCS are represented in blue and grey color respectively. Error bars correspond to
 669 the 95% confidence interval.



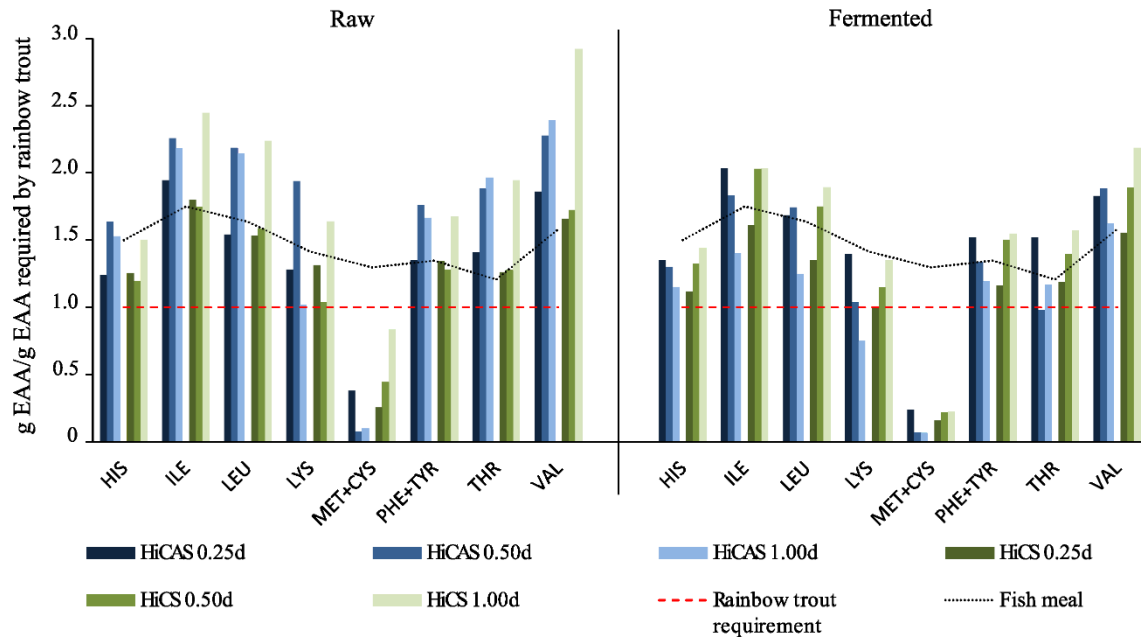
670

671 Fig. 3. A) Protein level as dry weight (DW), B) biomass productivities as g DW/L/d,

672 separated into protein and non-protein fraction. Error bars correspond to the 95%

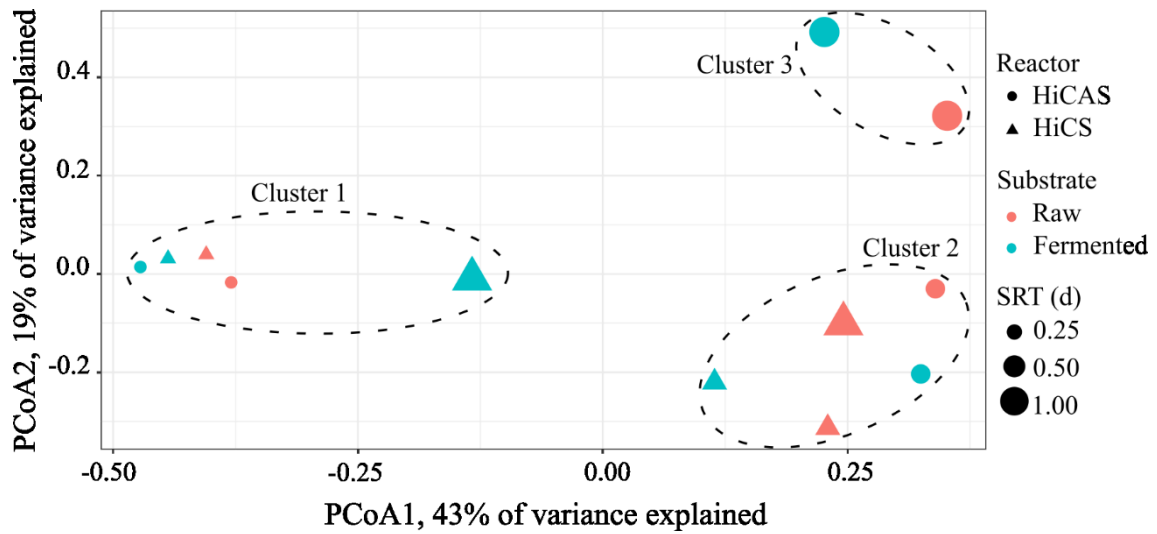
673 confidence interval. Asterisk "*" denotes a significant difference between the means

674 ($p < 0.05$).



675

676 Fig. 4. Essential amino acids (EAA) residuals of the AHB biomass in the 12 scenarios
 677 and fish meal normalized by the rainbow trout EAA requirement, represented by the red
 678 dashed line. The values equal or above 1 would meet or exceed rainbow trout's
 679 requirement. EAA abbreviations, HIS: histidine; ILE: isoleucine; LEU: leucine; LYS:
 680 lysine; MET+CYC: methionine+cysteine; PHE+TYR: phenylalanine+tyrosine; THR:
 681 threonine; VAL: valine.



682

683 Fig. 5. Principal Coordinate Analysis (PCoA) using Bray-Curtis distance for the
 684 comparison of the bacterial community similarities between the 12 tested scenarios.
 685 Each point represents one sample for a specific scenario. The closer the points are one
 686 another, higher the similarities between the microbial communities. The percentage of
 687 variation explained by each PCoA is indicated in axis.